

First published in:

Technologisch Instituut-K.VIV
Mechanical Separation and
Particle Technology

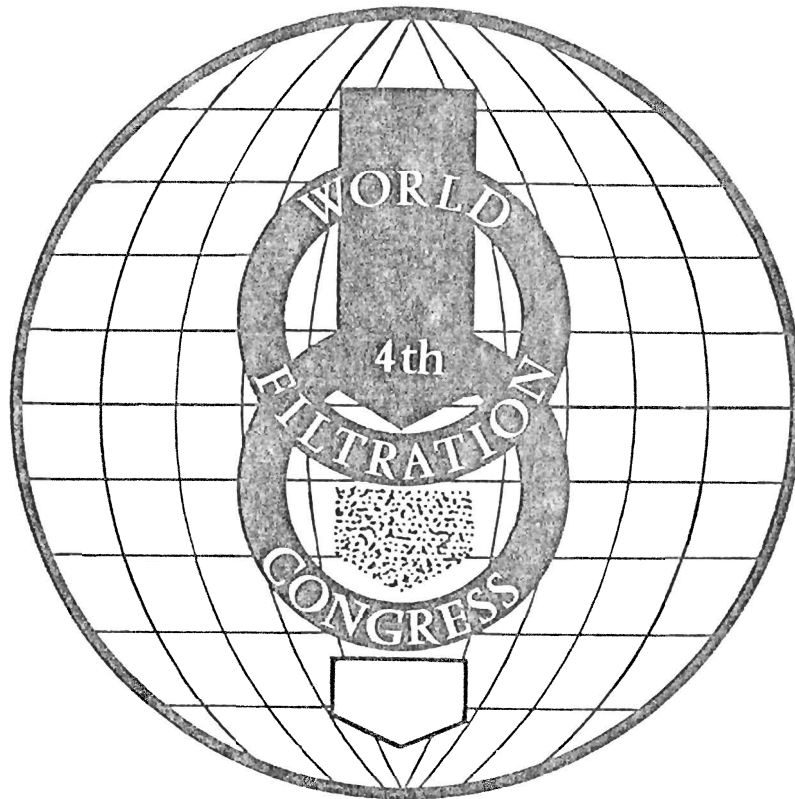
Volume 8

801)

Nur zum persönlichen Gebrauch

Vom Verfasser überreicht

PROCEEDINGS Part II



22 - 25 April 1986
Ostend, Belgium

Editors : R. Vanbrabant
J. Hermia
R.A. Weiler

The Royal Flemish Society of Engineers (K VIV) Antwerp (Belgium)
329th event of the European Federation of Chemical Engineers

EVA-STAR (Elektronisches Volltextarchiv – Scientific Articles Repository)
<http://digbib.ubka.uni-karlsruhe.de/volltexte/1000008950>

THE DISCHARGE OF FILTER CAKE BY AIR BLOW BACK; A MATHEMATICAL SIMULATION TO IMPROVE DESIGN AND OPERATION OF DISC FILTERS

Dipl.-Ing. R. Kern, Prof. Dr.-Ing. W. Stahl
Institut für Mechanische Verfahrenstechnik und Mechanik der
Universität Karlsruhe (TH), D-7500 Karlsruhe

ABSTRACT

The filter cake is discharged from the segments of rotary vacuum disc filters, usually by means of compressed air blow back. In order to operate the disc filter with high speed of rotation or to discharge an adhesive filter cake, it is necessary to optimize the design of the discharge equipment and the operating conditions.

Proceeding from equations describing the throughput of compressed air through the pipeline system of the disc filter, the pressure in the filter segment and the motion of the filter medium, the acceleration of the filter cake is calculated by a mathematical simulation. The influence of the design of the filter segment, the control head and the pipe diameter on the acceleration of the filter cake is discussed and possibilities to improve existing equipment of disc filters are shown.

Fig. 1 shows the operating principle of disc filter. It consists of a vertically arranged disc that turns about its axis of rotation, dipping with 40-50% into a suspension. The disc consists of individual filter cells in the shape of circular segments which are covered by a filter cloth.

During the rotational motion, the individual filter cells consecutively dip into the suspension. The filter cells are evacuated via a control mechanism. As a result of the vacuum in the filter cell, the suspension liquid flows through the filter cloth into the filter cell and from there through a piping system into a filtrate separator. A solid material is deposited on the filter cloth by a cake-forming filtration process and is carried out of the suspension together with the filter cell.

The cell emerges from the suspension during the further course of the rotational motion. Air from the environ-

ment of the filter cell is aspirated into it, thereby removing moisture from the filter cake.

This is followed by the removal of the filter cake from the filter cloth. For this purpose, compressed air is usually forced into the filter cell which tensions the filter cloth and the filter cake. When the filter cloth is taut, the cake dislodges and slides over a scraper into a solids chute. Cake and filtrate are disposed off separately.

Today, almost all filters operate with a plane control head (Fig. 1). In addition to the filter incorporating shafts with up to 12 filter discs filter with individual troughs and discs have been developed. The number of filter segments on a disc has been increased up to 30 and the thickness reduced. The typical rotational speeds of the filters are now much higher than before. Drive modules, which can be exchanged as compact units, are commonly used. For further information regarding the development and present standard of this filter technique, see [1,2,4,5,6,12,14, and 17].

The inexpensive design of the disc filter and its very large filter area in relation to its size have resulted in a wide field of application for the removal of solids from liquids, particularly in industries involved in the processing of coal, ferrous and non-ferrous metals [8,14,15].

This broad range of application of the disc filter is characterized by the fact that large mass flows of products with a low specific price/mass flow ratio can be processed. Thus, in order to be cost-effective, disc filter must attain high specific solids/filtrate throughputs [5,7,9,10,11,23,35]. Further developments of the disc filter to permit higher rotary speed and therefore to lower specific costs are essential.

of the filter-cell, in equilibrium with the elastic tensile stress of the filter cloth, which will be explained later.

An improvement of the cake discharge can be accomplished by means of constructive improvements to the inlet-valve geometry. An example of this is the rectangular valve, the area of which being plotted as curve 1, in Fig. 2, where the gradient can be observed to be significantly steeper. In order to improve older filters, constructed with a circular pipe overlap, the control zones can be subsequently modified to slot forms, or even better, as crescent, as can be seen in curve 2. These are not as favourable as the rectangular valves, but are better than circular/circular overlapping.

If the gas flow is conducted into a vacuum, or with high tank pressures, then as the line intersection begins, sound velocities are reached. The area of overlap is a linear term in equation 1 for the gas mass flow.

$$\dot{m} = \left(\frac{2}{\kappa+1}\right)^{\frac{1}{\kappa-1}} \cdot \rho^* \cdot \sqrt{\frac{2}{\kappa+1}} \cdot a_1^* \cdot A_{\ddot{u}} \quad (1)$$

After a substantial time-lapse, the gas flow rate is determined by the pressure-loss within the feed-pipes and control section. The area of overlap is a quadratic term in the calculation of the coefficient of resistance as in eq. 2.

$$\xi = (1 - A_{\ddot{u}}/A)^2 \quad (2)$$

The flow restriction is to be considered additionally. Fig. 3 illustrates the measured and calculated values for a radial control-valve incorporating circular/rectangular overlap cross-sections. The distribution of the pressure-drop for each machine element in % can be seen in Fig. 4. As a result of the deflection of the gas-flow inside the control-valve, its pressure-loss, when fully open, is relatively high.

FILTER CELL FILLING PROCEDURE

Gas flows into the filter cell while the control valve is open. This causes a built up pressure to be inside the filter cell relative to its environment. The volume of the filter cell and the gas flow rate determine the pressure rise rate. The pressure in the filter cell, which is affected by the gas flow, continues to increase until the filter cloth has been accelerated to such a

velocity that the volume increase of the filter cell corresponds to the volume flow of the gas. The filter cloth is then further accelerated while the pressure drops. The cloth attains its maximum velocity when the pressure difference between filtercell and environment becomes zero.

As a result of the filter cake/cloth velocity, the pressure falls below the environmental pressure. Filter cake and cloth then decelerate. The pressure decreases until the volume flow rate of the entering gas again corresponds to the filter cell volume increase. During the further deceleration of the filter cloth, the pressure increases to that of the environment and the procedure starts again from the beginning.

The oscillation thus created, whose frequency and amplitude are dependent on the magnitude of the gas flow, the volume of the filter cell, compressibility of the gas and the mass of the filter cake. This oscillation is superposed upon the translatory motion. In each case the velocity of the translatory motion is the time-related average value of the local cloth velocity. The velocity, averaged in time and over the filter surface, results from the volume increase of the filter cell with respect to the filter surface.

As the distance increases, the motion of the filter cloth is affected by elastic forces caused by the tensioning of the filter cloth. This gives rise to interference oscillations which are dependent upon the filter cell geometry. A minor damping action is caused as a result of energy dissipation in the filter cloth. A significant energy loss is, however, produced by the gas stream which escapes to the environment through the filter cake, particularly then, when cake cracking occurs. The filter cloth oscillation is strongly damped by the escaping compressed air. Further, the oscillation cycle is technically unimportant. One relevant aspect is the fact that the pressure in the filter cell - when the cloth is almost stationary - increases to such an extent that the cake is detached by the filter cell pressure. In some filter cakes, this detachment procedure is additionally supported by a filtrate emergence from the filter cloth, reducing the adhesive stresses between the filter cake and the cloth.

The following section presents the differential equation for the computation of filter cloth motion. It is solved numerically and indicates a complex dynamic behavior due to the

A new application area for the disc filter is expected in the field of pressure filtration [20,30,31,32]. In such applications, the disc filter possesses other advantages due to its low space requirements and the ability to accommodate large filter areas inside expensive pressure vessels.

To attain the objectives, it is necessary to be able to forecast with certainty how the filtration, dewatering and filter cake discharge processes will behave. The theory of filtration and moisture removal has been dealt with in a number of publications [3,5-36] and are not within the scope of this paper which mainly considers the influence of designed parameters on filter cake discharge.

Reliable removal of the filter cake is of great importance, particularly concerning filters operating in pressurized chambers. Since pressurized chambers are not readily accessible, problems with the removal of the filter cake can impair the operation or even cause a failure of the filter unit. However, even in conventional filters, removal problems may occur, causing a deterioration of throughput and poor residual moisture levels.

DESCRIPTION OF FILTER CAKE DISCHARGE

Adhesive forces cause the filter cake to cling to the filter cloth. These forces must be overcome to permit removal of the filter cake. For this purpose, in disc filters, compressed air from a reservoir is blown in the opposite direction to the filtrate flow through the filtrate piping into the filter cell. This procedure is known as cake discharge by compressed air. The pressure developed in the filter cell in this manner accelerates the filter cloth and the cake adhering to it. After moving a distance of a few mm to a few cm, the filter cloth is tensioned and decelerates with the adhering filter cake. The reduced speed of the filter cloth causes a pressure increase in the filter cell. Simultaneously, inertia forces appear in the filter cake and compressional forces act at its bottom surface, releasing it from the filter surface, provided that the adhesive forces are exceeded.

AIR FLOW THROUGH THE DISC FILTER

For the time being, the compressed air is stored in a reservoir whose volume should be several times that of the

filtrate pipe and cell. The compressed air line is under pressure as far as the control head. The passage into the filter pipe system is opened to the compressed air in a manner dependent on the rotary speed of the filter and on the control geometry. In many disc filters a magnetically activated quick-opening valve is fitted in the compressed air line before the control head. This valve is intended to ensure rapid opening of the compressed air line particularly in the case of slowly rotating filters.

The air flows through the control head and the filtrate pipe up to the filter cell. The filtrate pipe should be short and have as few bends as possible. An adequate diameter should be selected. The mass flow of the gas is dependent on these design characteristics and on the operating conditions of the filter.

The gas extraction is initiated by the opening of the control head. In the simplest case, this is executed by intersecting the filtrate feed-pipe, with the compressed-air line. Providing both pipes are of circular cross-section, the area of intersection corresponds to that of two overlapping circles. This area (curve 3) is plotted in Fig. 2 as a function of the overlap, which at the instant that the valve is opened, possesses a low gradient.

As to be shown later, it is necessary for the gas flow to be as high as possible when attaining the outside pressure of the filter cell. For this purpose, the time required to fill the cell to the pressure of its vicinity can be exploited. The higher the angular velocity of the filter, the larger is the intersection area during this time-lapse, and the steeper is the function of the intersection angle. The angular velocity may not, of course, exceed the overlap maximum within this interval.

In order to save time and compressed-air necessary to fill the filter cell, an improvement of the discharge has been attempted, by filling the cell to its environmental pressure before introducing the compressed-air pulse. In this case, at the instant that the valve begins to open, the filter cloth movement is initiated, at the area of intersection O , and at the lowest function of intersection area gradient. A pre air-bleeding of the filter cell is, therefore, for the discharge, often not advantageous, but disadvantageous. An exception of this, however, exists when the filter cake removal is not accomplished through, or with the aid of inertia forces, but owing to the internal pressure

transition of waves, interference oscillations due to differing chord lengths and the interaction between filter cloth motion and gas flow as already mentioned above. However, within the scope of this paper, the dynamic procedures are only briefly reviewed. Instead, concrete design influences from equilibrium states of the filter cloth are examined in some detail.

FORCE EQUILIBRIUM ON THE FILTER CELL

The forces acting on the filter cloth are shown in Fig. 5. These are the forces caused by the differential pressure P between the filter cell and the environment, the elastic forces in the filter cloth in warp K and weft S directions, and the inertial force T on the filter cake. Gravitational force is neglected. The corresponding force equations are in z -direction:

$$d^2 F_P = \Delta p \cdot r \cdot d\varphi \cdot dr \quad (3)$$

for the force due to the pressure

$$d^2 K = \epsilon_r \cdot E_r \cdot \frac{\partial^2 z}{\partial r^2} \cdot r \cdot d\varphi \cdot dr \quad (4)$$

for the warp cloth force

$$d^2 S = \epsilon_\varphi \cdot E_\varphi \cdot \frac{\partial^2 z}{\partial \varphi^2} \cdot \frac{1}{r} \cdot dr \cdot d\varphi \quad (5)$$

for the weft cloth force

$$d^2 F_T = - m \cdot \frac{\partial^2 z}{\partial t^2} \cdot r dr \cdot d\varphi \quad (6)$$

for the inertial force. The force equilibrium in the z direction yields the differential equation.

$$m \cdot \frac{\partial^2 z}{\partial t^2} = \Delta p + \epsilon_r \cdot E_r \cdot \frac{\partial^2 z}{\partial r^2} + \epsilon_\varphi \cdot E_\varphi \cdot \frac{1}{r^2} \cdot \frac{\partial^2 z}{\partial \varphi^2} \quad (7)$$

with the elongation of the radial direction

$$\epsilon_r = \left| \int_0^1 \sqrt{1 + \left(\frac{\partial z}{\partial r}\right)^2} \cdot dr - 1 \right| \cdot \frac{1}{l_0} \quad (8)$$

and the angular elongation

$$\epsilon_\varphi = \left| \int_0^{\varphi_0} \sqrt{1 + \left(\frac{\partial z}{\partial \varphi}\right)^2} \cdot d\varphi - \varphi_0 \right| \cdot \frac{1}{\varphi_0} \quad (9)$$

The differential pressure results from the mass flow into the filter cell and from the ideal gas law

$$\Delta p = \frac{R \cdot T \cdot (m_{L0} + \int_0^t (\dot{m}_{L1} - \dot{m}_{L2}) \cdot dt)}{V} \quad (10)$$

FILTER CLOTH STATIC EQUILIBRIUM

The bulge distortion of the filter cloth is accompanied by elastic stresses in the described manner. In a static elasticity calculation for the filter cloth, i.e. neglecting the inertial forces in equation 7, the elastic stresses in the cloth are in equilibrium with the pressure in the filter cell. Provided the dynamic effects on the geometric structure of the filter cloth are ignored, this equilibrium pressure corresponds to an average tension component developed by the filter cloth to counteract the pressure in the filter cell and the inertial forces of the filter cake.

Providing that the pressure component is not reduced because of its ability to act on only a limited portion of the bottom surface of the filter cake as a result of the pore structure.

The magnitude of these stresses also corresponds to the filter cake stress caused by pressure and inertial forces. A curve of this equilibrium pressure plotted over the space and volume of the filter cloth is a significant parameter for the detachment of the filter cake. The influence of several filter cell parameters on this distribution will be discussed below.

EFFECTS OF THE CELL ANGLE

In Fig. 6 the pressure in the filter cell is shown as a function of the bulge volume of the filter cloth. The curves shown in the diagram vary with the angle of the filter cell. It can be clearly seen that as the angle of the filter cell increases, the quantity of air that is necessary for the attainment of a desired cell pressure level increases also. Thus, with the same filter cell piping, large cell angles require longer control valve opening

times or lower filter speeds and greater quantities of compressed air. The reason for this behavior is that the forces directed vertically onto the filter cloth can only be absorbed by a curvature of the cloth, the radius of which decreasing with increasing restraint length.

For existing filter cells with large centric angles, this can be remedied by reducing the restraint length of the filter cloth, by attaching strips to the filter cell to hold the cloth down.

These strips can traverse the filter cell either laterally or longitudinally. Fig. 7 shows the extensions in a longitudinal direction plotted against those in the lateral direction. The extensions in the longitudinal direction plotted against those in the lateral direction. It can therefore be advisable to attach strips to the filter cell on a transverse direction in order to increase the stresses in the longitudinal fibres of the filter cloth so that they can also significantly contribute to the deceleration of the filter cloth instead of the transverse fibres only which would otherwise prematurely break.

EFFECT OF THE MODULES OF ELASTICITY

The pressure in the filter cell is plotted against the displacement volume for filter cloth modulus of elasticity between 1×10^5 and 1×10^6 N/m in Fig. 8. The diagram indicates that the modulus of elasticity can contribute significantly to the rapid increase of the cell pressure. In the case of an inadequate compressed air supply configuration, the selection of a filter cloth with a large modulus of elasticity can result in an improvement in cake discharge.

EFFECT OF PRETENSIONING THE FILTER CLOTH

The filter cloth can be tensioned in the longitudinal or transverse direction or can be left loose. Fig. 9 shows an example for pretensioning in the transverse direction. The cell pressure is again plotted against the bulge volume of the filter cloth. The mean curve represents the typical case of the filter cloth lying flat on the filter cell without pretensioning. If the cloth is stretched about 1%, an appreciably more rapid pressure increase takes place. This can be advantageous for

an underdimensioned compressed air supply. The cloth, whose angle is about 0.5% larger than the cell angle, can also be advantageous. It offers a wide range in which the pressure hardly increases. A high filter cloth speed can be attained in this range which, as a result of the abrupt change of direction with a pronounced pressure increase, results in a rapid filter cloth deceleration. However, for this purpose, large quantities of compressed air must be available over a relatively long period of time.

Fig. 10 shows the pretensioning in a longitudinal direction. It shows that in this case, a noticeable effect is only obtained with impracticably high pretensioning values. In order to attain other results, the longitudinal direction of the filter cloth must be subdivided. However, it must be mentioned that the pretensioning values in both the transverse and longitudinal directions are limited by the plastic flow of the filter cloth.

EFFECTS OF THE CELL VOLUME

All the factors discussed have one thing in common. In all cases, a filter cake discharge improvement was achieved in that the curve slope of the pressure increase relative to the filter cell volume became steeper. In other words, a higher pressure was developed in the filter cell with the same quantity of compressed air. In Fig. 11 the volume of the 33° test cell is plotted against the pressure in the filter cell. The continuous curve represents the equilibrium condition. Triangular symbols indicate the theoretical curve geometry when the inertial forces are taken into account. Apart from the oscillations at the start of the cycle, the pressure curve virtually follows the shape of the equilibrium curve. In the case of the respective filter cell, only the attainable pressure is significant. The inertial forces correspond to the deviation of the symbols from the equilibrium curve and are negligibly small.

In the case of large gas flow rates or small cell volumes, oscillation around the static equilibrium occur (Fig. 12) due to the inertia forces. The pressure variation from static equilibrium in the filter cell, acting upon the filter cake, conforms with the area inertia as calculated by eq. 5. In this instance, inertia forces must be taken into consideration.

EXPERIMENTAL RESULTS

Fig. 13 shows experimental results for cell angles of 33° , 22.5° and 10° . The abscissa represents the pressure in the compressed air reservoir and the ordinate the mass ratio of filter cake discharge to filter cake disposition. The 10° cell begins to discharge at a pressure of 0.4 bar and throws the filter cake off completely at 1.3 bar. The 33° cell only starts to discharge at 2.3 bar and will not throw off the entire filter cake below 3.0 bar.

Fig. 14 shows the removed cake fraction plotted against the discharge pressure for the 33° cell with and without cloth restraint. An improvement of the filter cake discharge can be seen. Due to the considerable border length of the attached strip on the relatively small filter surface of the test cell, the filter cake - even though it has been completely detached from the filter cloth - is still retained by the strip. Thus, the improvement in the diagram is less pronounced than it would be in the case of larger filter cells.

Fig. 15 shows the experimental results for a pretensioned filter cloth. The pressure required for a complete discharge is reduced by about 0.5 bar when the filter cloth is pretensioned.

An experiment in which the filter cell was filled with spheres in order to reduce the cell volume is shown in Fig. 16. The pressure for 100% discharge from the cell whose volume was reduced by 45% is considerably lower than the pressure required for 100% discharge of the unfilled filter cell.

SUMMARY

The article shows that the pressure variation in a filter cell, in which relatively low air streams are applied, corresponds to the equilibrium pressure needed to bulge the filter cloth to a particular bulge displacement volume. In these cases, the variation of the equilibrium pressure with the filter cloth bulge volume is significant. This is the case in many currently operating disc filters.

However, in the case of filter cells of small volume or with large gas flows, inertia forces are significantly involved in cake release.

LITERATURE

- |1| Marktübersicht über Filterapparate Chemie-Ingenieur-Technik 55, 11, p. 539-557, 1983/11
- |2| Alt, C. Entwicklungstendenzen der Filtertechnik, Chemie-Ingenieur-Technik 55, 11, p. 536-538, 1983/11
- |3| Bolek, M. Bestimmen eines Filtrationszyklus für kontinuierlichen Vakuumprozess Maschinenmarkt 81, p.1134-1137, 1975
- |4| Gösele, W. Filterapparate - Eine Übersicht Aufbereitungstechnik 1977/5
- |5| Stahl, W. Die Grenzen der Steigerung von Durchsatz und Trenneffekt bei Vakuumdrehfiltern und ihre Einflüsse auf die Konstruktion, Vortrag Achema 1979
- |6| Stahl, W., Kern, R. Neuere apparative Entwicklungen bei kontinuierlichen Vakuumfiltern - Möglichkeiten der Anpassung und Verbesserung älterer Filter GVC-Tagung Filt.techn., Wiesbaden 1983
- |7| Tiller, F.M., Crump, J.R. How to Increase Filtration Rates in Continuous Filters, Chem. Eng. 6, p. 183-187, 1977/1
- |8| Merker, K.J. Vergleichende Untersuchungen an Handfiltern und Großtechnischen Vakuumscheibenfiltern zur Bestimmung der Filtrationswiderstände und der Filtrationsleistung Dissertation Universität München 1982
- |9| Rushton, A. Design Throuputs in Rotary Disc Vacuum Filtration with Incompressible Cakes, Powder Technology 21, p.161-169, 1978
- |10| Stahl, W. Vergleich der Anwendungstechnik und der Betriebskosten von Hochleistungs-scheibenfiltern und konventionellen Trommelfiltern, Vortrag Achema 1976
- |11| Stahl, W. Cost/Performance Comparison between Disc- and Drumfilters, Filtr. & Sep. 1978/1

- | 12 | Stahl, W.
Design and Comparison of Technical Aspects to Conventional Multi Disc Filters
Solid-Liquid-Separation Symposium at Johannesburg, 1978
- | 13 | Stahl, W.
Operating Conditions of Krauss-Maffei Disc-Filter for different Applications
Solid-Liquid Separation Symposium Johannesburg, 1984
- | 14 | Stahl W., Breuer, U., Krappmann, F.
Ein neuartiges Scheibenfilter für die Massengut-, Aufbereitungsindustrie, Erzmetall 32, p. 69-71, 1979
- | 15 | Stahl, W., Reinsperger H, Stockhausen, W.
Application of Disc Filters in the Bayer Process Alumina and Bauxite Production, Appl. of the Metallurgical Society of AIME, Light Metall 1, 1979
- | 16 | Tiller, F.M., Risbud H.
Analytical Formulas for Disc Filters
AIChE J. Vol. 20, 1, p. 36-43, 1974
- | 17 | Wetzel, B.
Neueste Erkenntnisse beim Einsatz von Scheibenfiltern, Chemie, Anlagen Verfahren 10, 1973
- | 18 | Wetzel, B.
Disk-Filter Performance Improved by Equipment Re-Design, Filtr. & Sep. 11, 3, 1974
- | 19 | Baluais, G., Dodds, J., Tondeur, D.
Die Kinetik der Verdrängungswässerung in Filterkuchen: Eine analytische Näherung
Powtech '83: Particle technology, Institution of Chemical Engineers, Symposium Series No. 69, p. 101-121 1983/3
- | 20 | Bott, R., Anlauf, H., Stahl, W.
Kontinuierliche Druckfiltration feinstkörniger Kohlekonzentrate Aufbereitungstechnik, 1984/5
- | 21 | Bott, R., Stahl, W.
Improvement of the Residual Moisture Content by Hyperbar Vacuum Filtration
Solid/Liquid Symposium of the Filtration Society, 1984/4
- | 22 | Bruk, O.L.
Allgemeine Gesetzmäßigkeiten des Filterns von Kohlensuspensionen
Koks i Chimija, Moskva, p.5-8, 1984
- | 23 | Carleton, A.J., Mehta, K.B.
Blatt-Test-Vorhersagen und die großtechn. Leistung von Vakuumfiltern
Filtration & Separation, Croydon 21, p. 55-57, 1984/1
- | 24 | Kuxmann, U.
Die Verarbeitung von komplexen Erzen und sekundären Rohstoffen aus verfahrenstechnischer Sicht
Erzmetall, Band 31, 9, p. 381-442 1978
- | 25 | Kämpf, F.
Untersuchungen an Drehfiltern bei der Filtration von Rotschlamm
Aluminium 45, p. 473-476, 1969
- | 26 | Kämpf, F., Tusche, J.
Erfahrungen bei der Filtration von Rotschlamm auf Drehfiltern
Erzmetall 20, p. 406, 1967
- | 27 | Osgood, Geoffrey M.A. (Cantab), F.R.I.C., C.I.Mech.E.
Filter Sheets and Sheet Filtration
Filtration & Separation, 1967/7
- | 28 | Redeker, D., Steiner, K.-H., Esser, U.
Das mechanische Entfeuchten von Filterkuchen, Chem.-Ing.Techn.55, 11, p.829-839, 1983/11
- | 29 | Rushton, Hameed
The Effect of Concentration in Rotary Vacuum Filtration
Filtration & Separation 2, 136-139, 1977
- | 30 | Stahl, W., Anlauf, H., Bott, R.
Physikalische Grundlagen der mechanischen Flüssigkeitsabtrennung durch Filtration, GVC-Tagung Filtr.techn., Wiesbaden, 1983/4
- | 31 | Stahl, W., Anlauf, H., Bott, R.
Eine neue Methode zur Entwässerung feiner Massenprodukte
112 th AIME Meeting, Atlanta, 1983
- | 32 | Stahl, W., Anlauf, H., Bott, R.
Entwässerung von Erzkonzentraten - Wege zur weiteren Restfeuchteminderung, Erzmetall 1983/6
- | 33 | Stahl, W., Bott, R., Anlauf, H.
Druckfiltration von Eisenerztrüben
Aufbereitungstechnik 5, p. 243-251, 1983/5
- | 34 | Wakeman, R.J.
Low Pressure Dewatering Kinetics of Incompressible Filter Cake, Int.J. of Min.Proc. 5, p. 395-405, 1979

- |35| Wakeman, R.J.
 Filtrieren und Waschen auf Vakuum-
 filtern - wirtschaftliche Pro-
 zeßoptimierung
 Filtration & Separation, Corydon 21,
 p. 201-205, 1984/5
- |36| Willis, M.S.
 A multiphase theory of filtration
 In: Wakeman, R.J.: Progress in
 filtration and separation 3, Amster-
 dam: Elsevier, 1983, 1-56
- |37| Zoebel, H., Krutschik, J.
 Strömung durch Rohre und Ventile
 Springer Verlag, 1978
- |38| Kern, R. Stahl, W.
 The Discharge of Filter Cakes
 Solids/Liquids Symposium of the
 Filtration Society 1984/4

FORMULAE

a^*	sound velocity	$ \text{m/s} $
A^1	area	$ \text{m}^2 $
A_{ij}	intersection area	$ \text{m}^2 $
E	elasticity modulus	$ \text{N/m} $
F	force	$ \text{N} $
K	warp cloth force	$ \text{N} $
m	filter cake mass per area	$ \text{kg/m}^2 $
l	filter cell length	$ \text{m} $
m_{Lo}^o	initial mass of gas in the filter cell	$ \text{kg} $
\dot{m}_{L1}	gas flow into the filter cell	$ \text{kg/s} $
\dot{m}_{L2}	gas flow out of the fil- ter cell	$ \text{kg/s} $
P	pressure	$ \text{N/m}^2 $
R	gas constant	$ \text{J/kg}^o\text{K} $
r	coordinate	$ \text{m} $
S	welt cloth force	$ \text{N} $
T (index)	inertia	$ \text{m}^2 $
T	temperatur	$ \text{K} $
t	time	$ \text{s} $
V	volume of filter cell	$ \text{m}^3 $
Z	coordinate	$ \text{m} $
Δ	difference	$ - $
ϵ	elongation	$ - $
	coordinate	$ \text{m} $
ρ	density	$ \text{kg/m}^3 $
κ	polytrope coefficient	$ - $

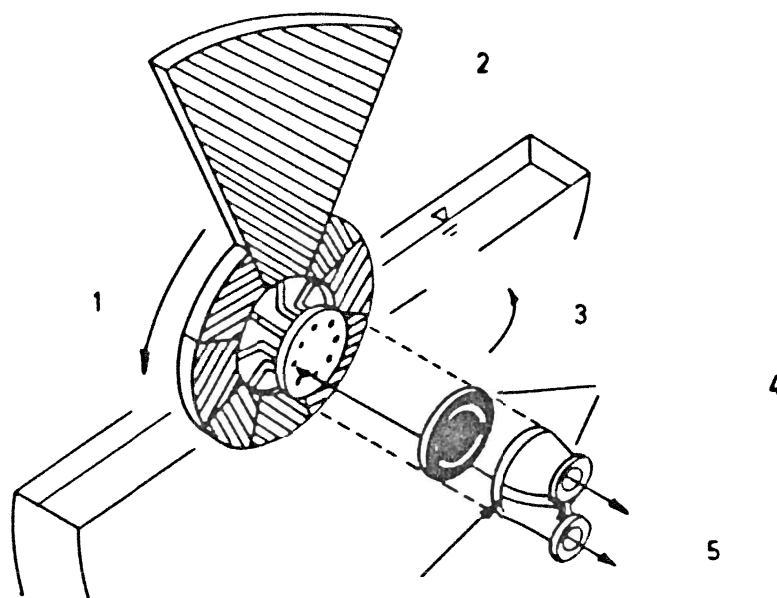


Figure 1:

 Principle of disc filter apparatus

- 1 Discharge of filter cake
- 2 Dewatering
- 3 Cake formation
- 4 Pressure pipe
- 5 Control head

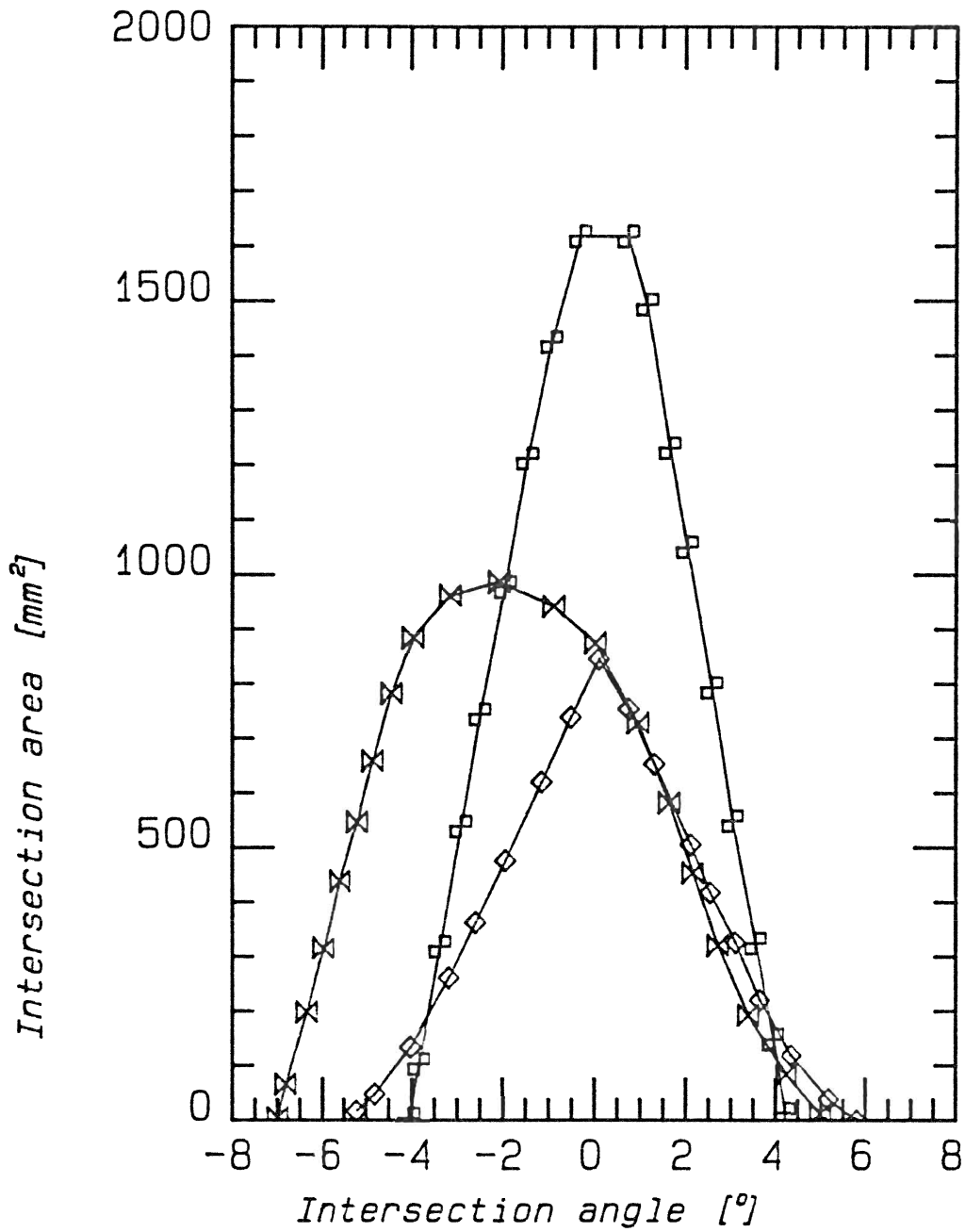


Figure 2:

 Different control head geometries

- ▣ retangle (1)
- ✕ crescent (2)
- ◇ circle (3)

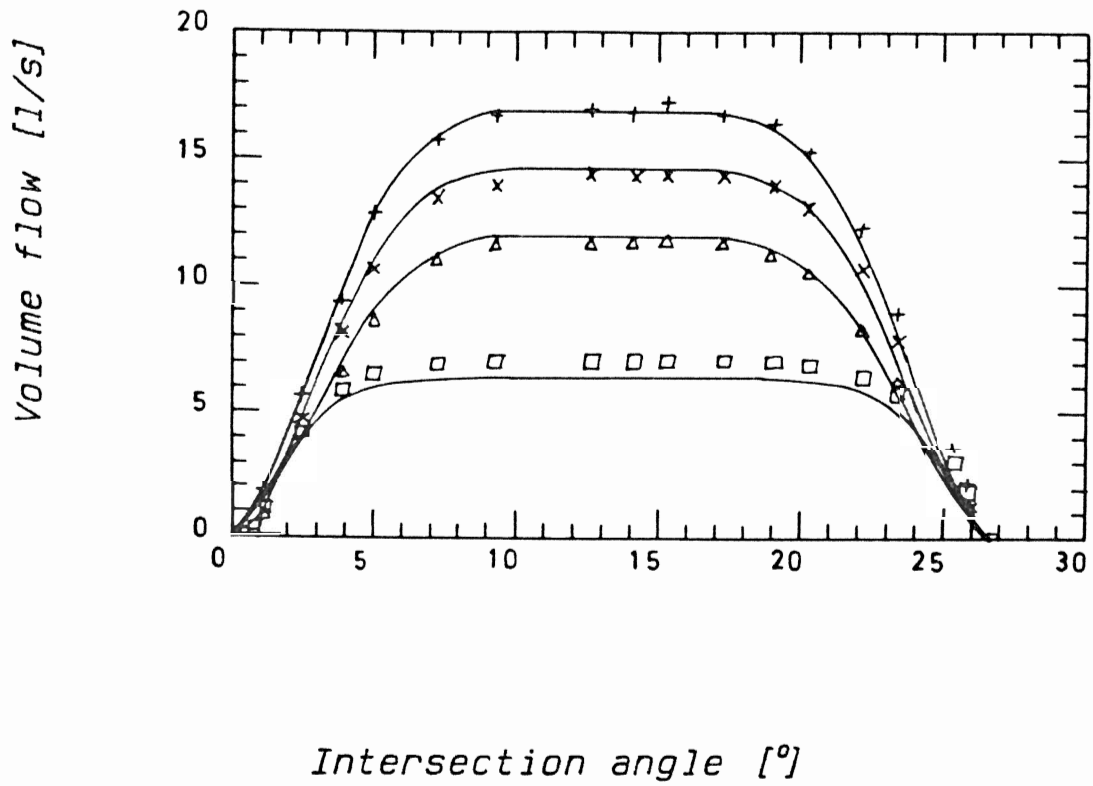


Figure 3:

Volume flow as a function fo intersection angle

+ 0.20 Bar

x 0.15 Bar

Δ 0.10 Bar

□ 0.05 Bar

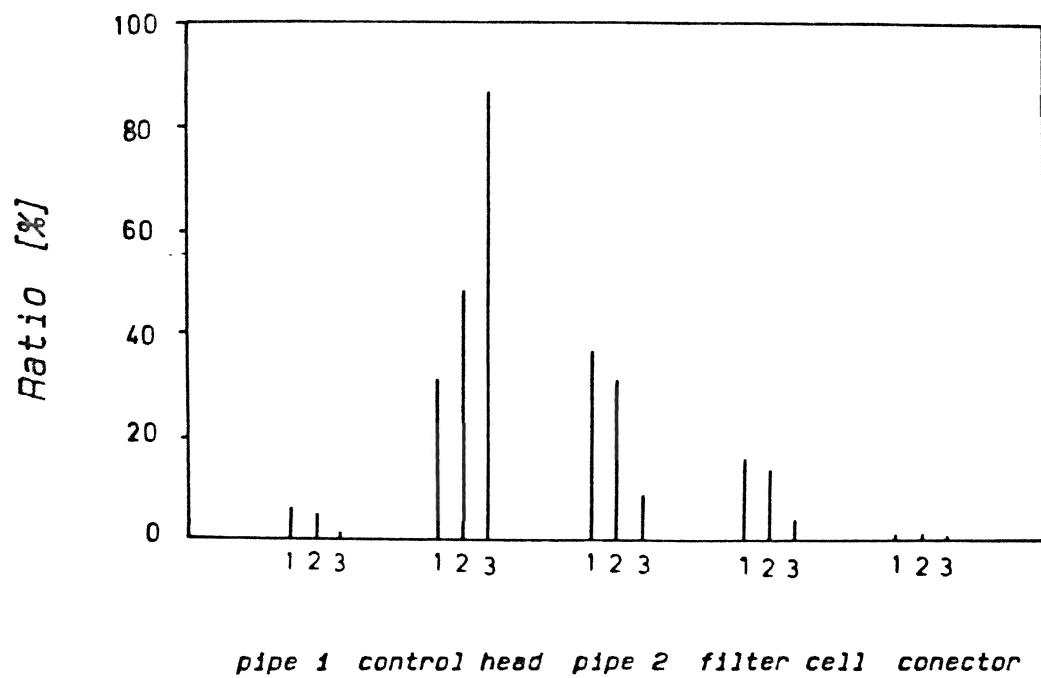


Figure 4:

Ratio of flow resistance

1 open

2 half open

3 quarter open

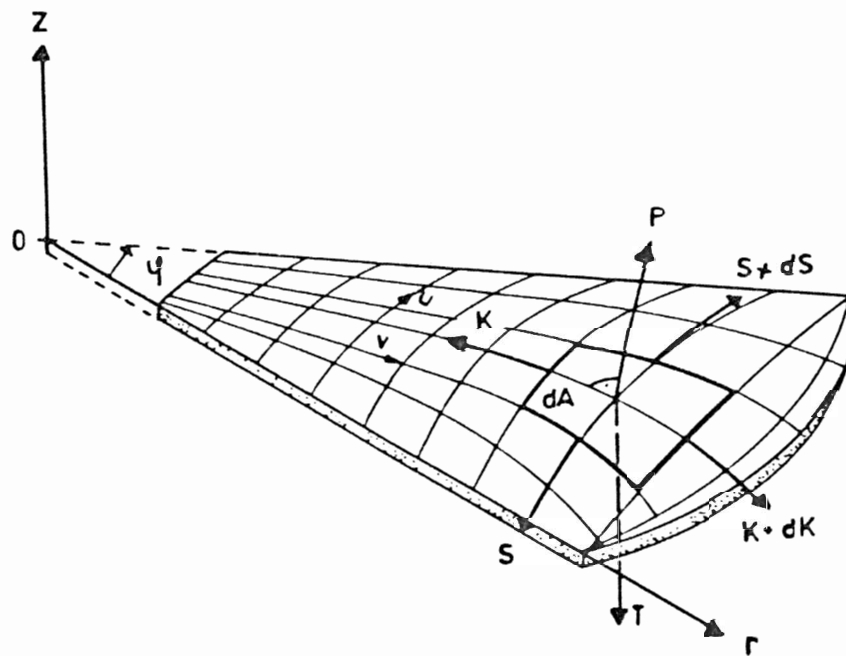


Figure 5:

 Forces acting on the filter cloth

- P : Pressure
- S, K : Elastic forces
- T : Inertia force
- u, v, r, φ : Coordinates
- dA : Differential area

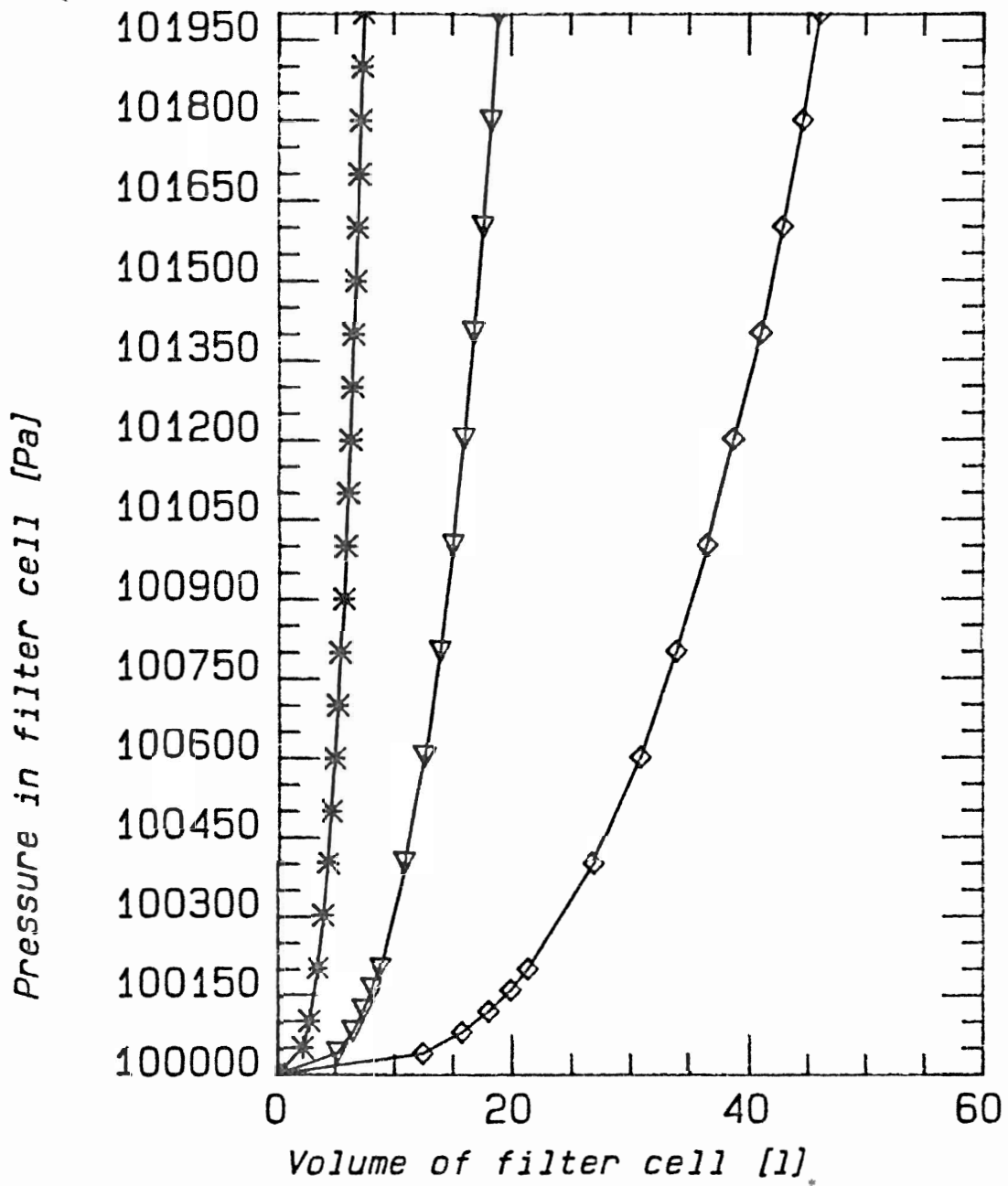


Figure 6:

Influence of filter angle

* 12 Grad

▽ 20 Grad

◇ 30 Grad

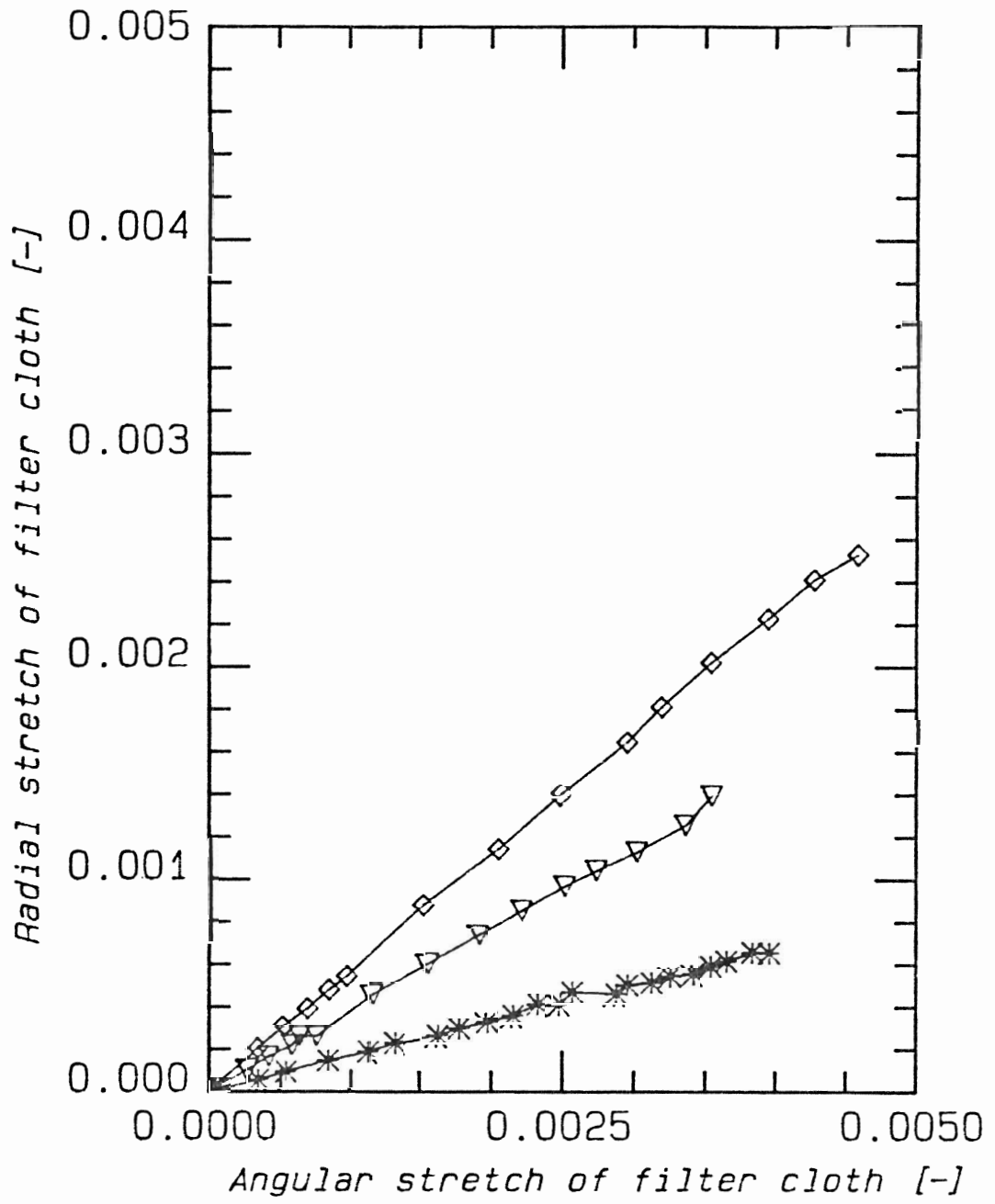


Figure 7:

 Influence of filter angle

- * 12 Grad
- ▽ 20 Grad
- ◇ 30 Grad

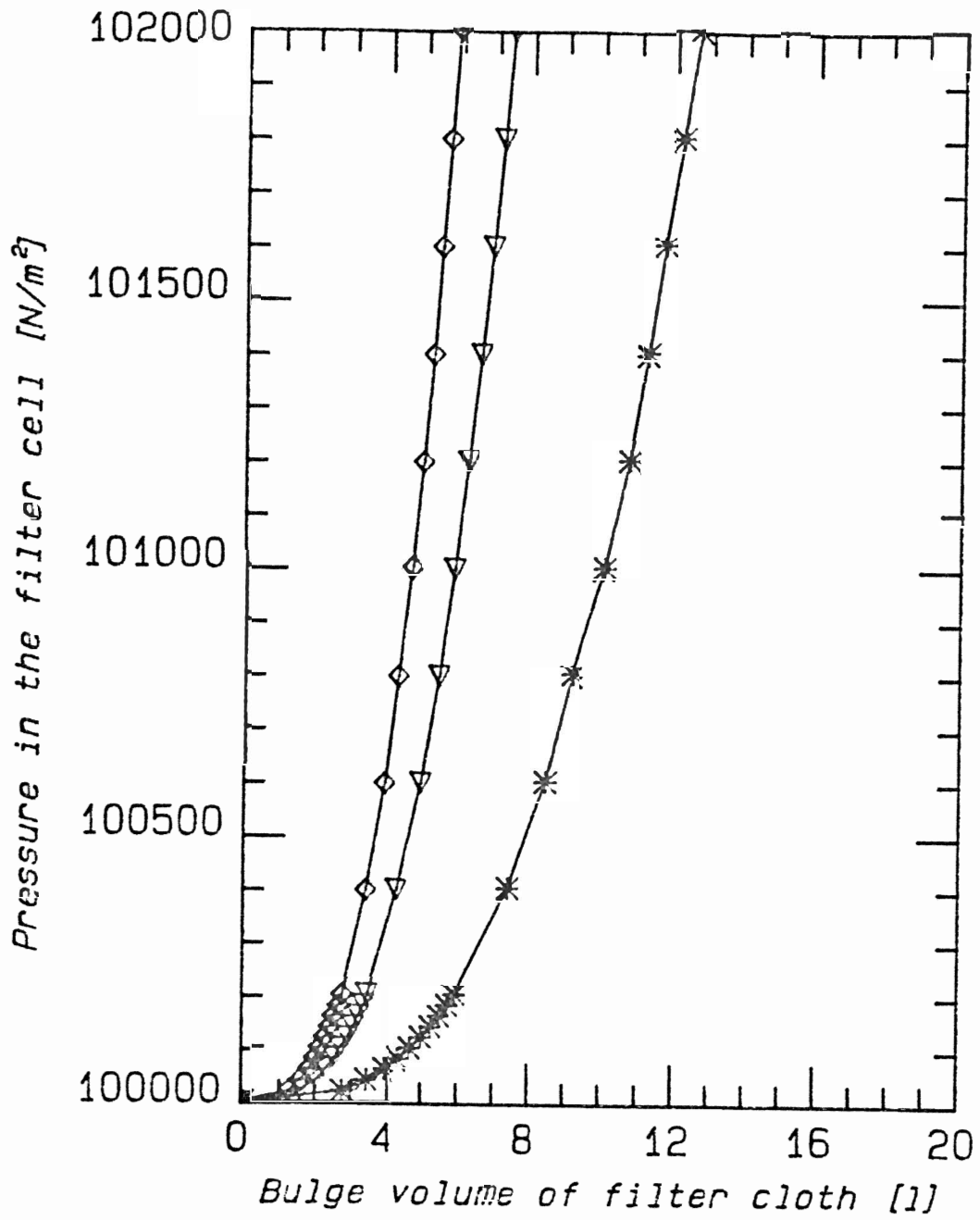


Figure 8:

 Influence of the modulus of elasticity

Modulus of elasticity

* 1×10^5 [N/m²]

▽ 5×10^5 [N/m²]

◇ 1×10^6 [N/m²]

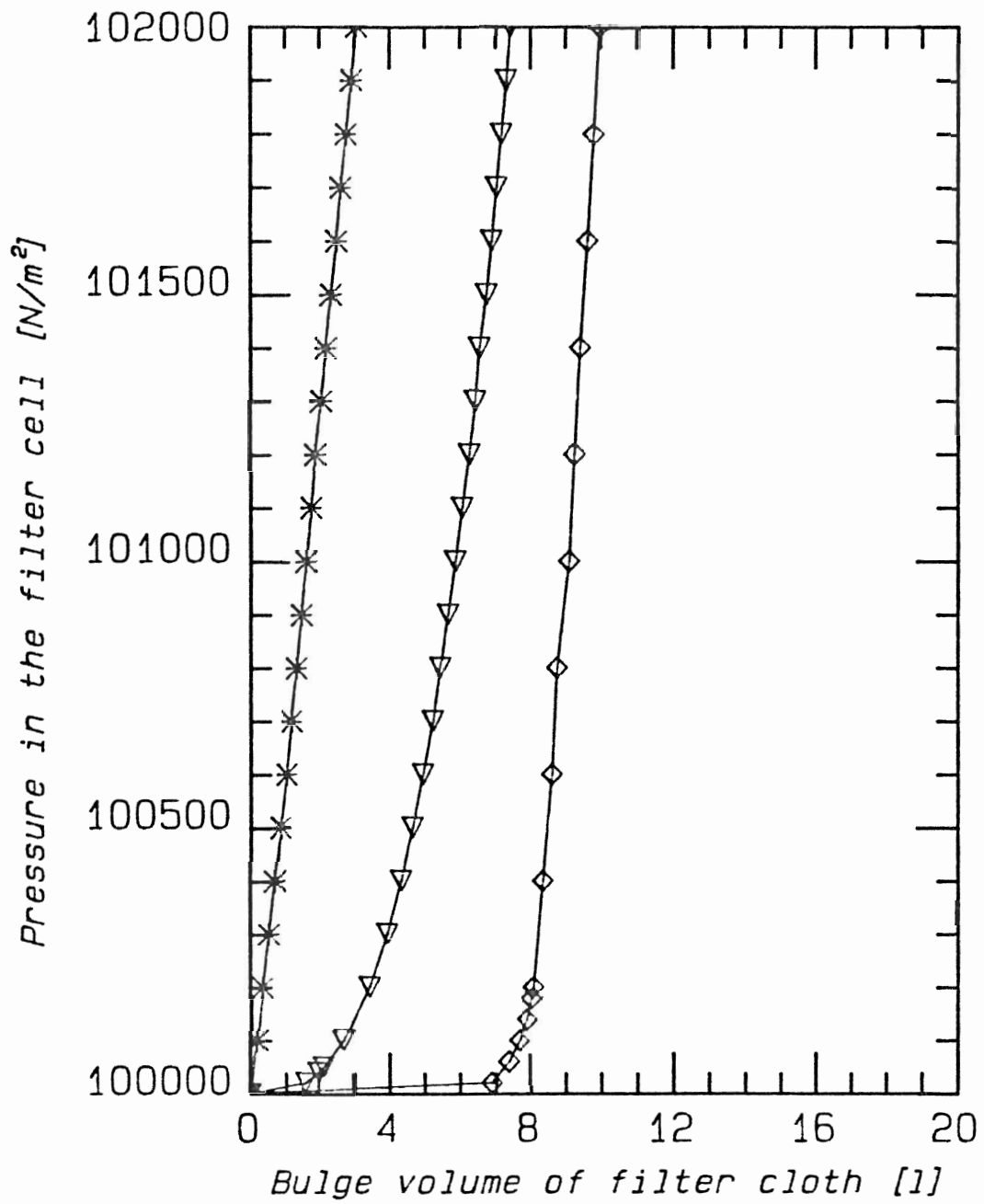


Figure 9:

Influence of initial angular stretch

Initial stretch

- * .9 [%]
- ▽ .0 [%]
- ◇ -.5 [%]

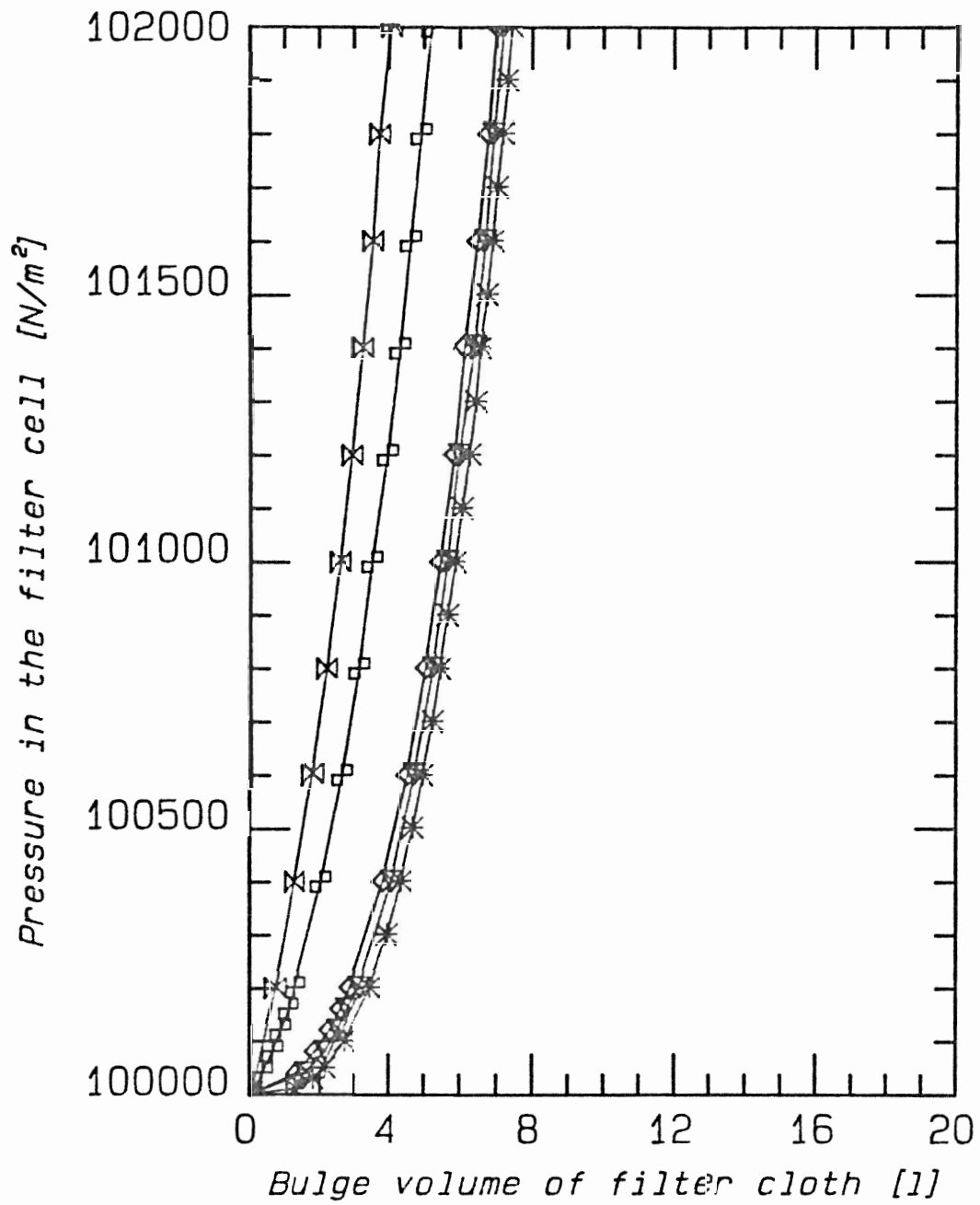


Figure 10:

 Influence of initial radial stretch

Initial stretch

- * .0 [%]
- ▽ .3 [%]
- ◇ .6 [%]
- 6.0 [%]
- ⊠ 13.0 [%]

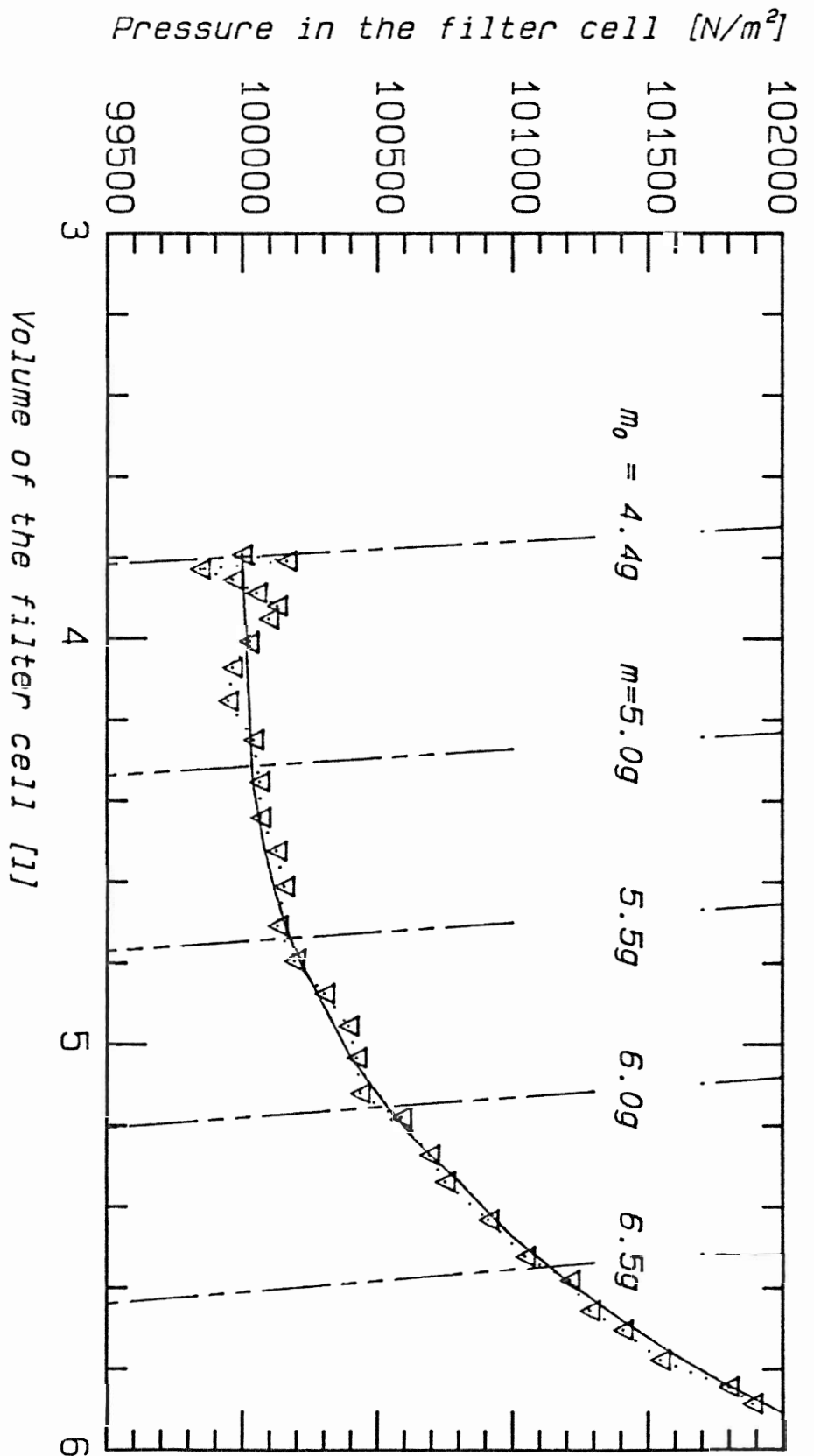


Figure 11:

 Experimental cell with 33° angle
 — static balance
 ▼ gas mass flow 0.008 kg/s

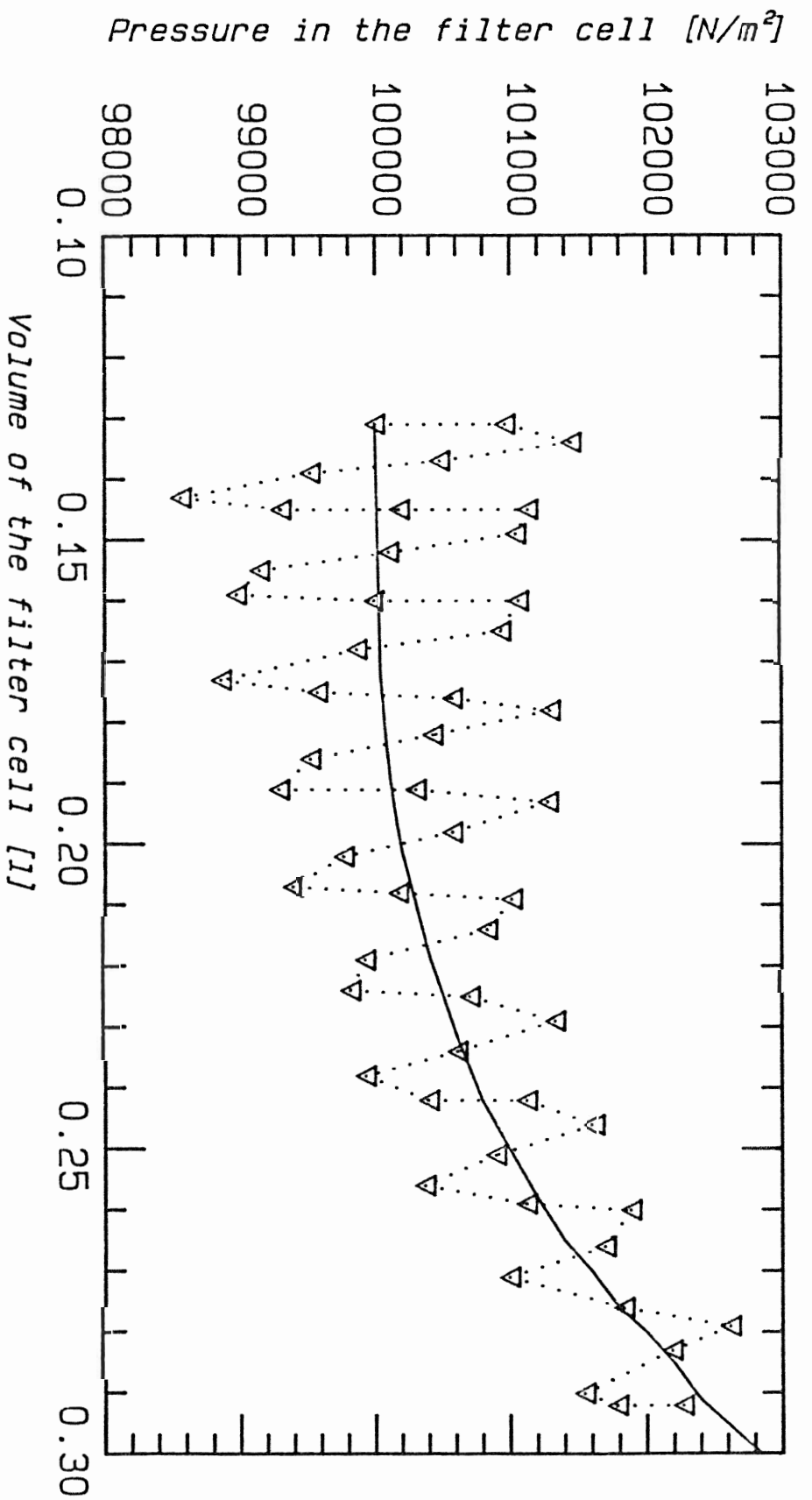


Figure 12:

 Experimental cell with 10° angle
 — static balance
 ∇ gas mass flow 0.008 kg/s

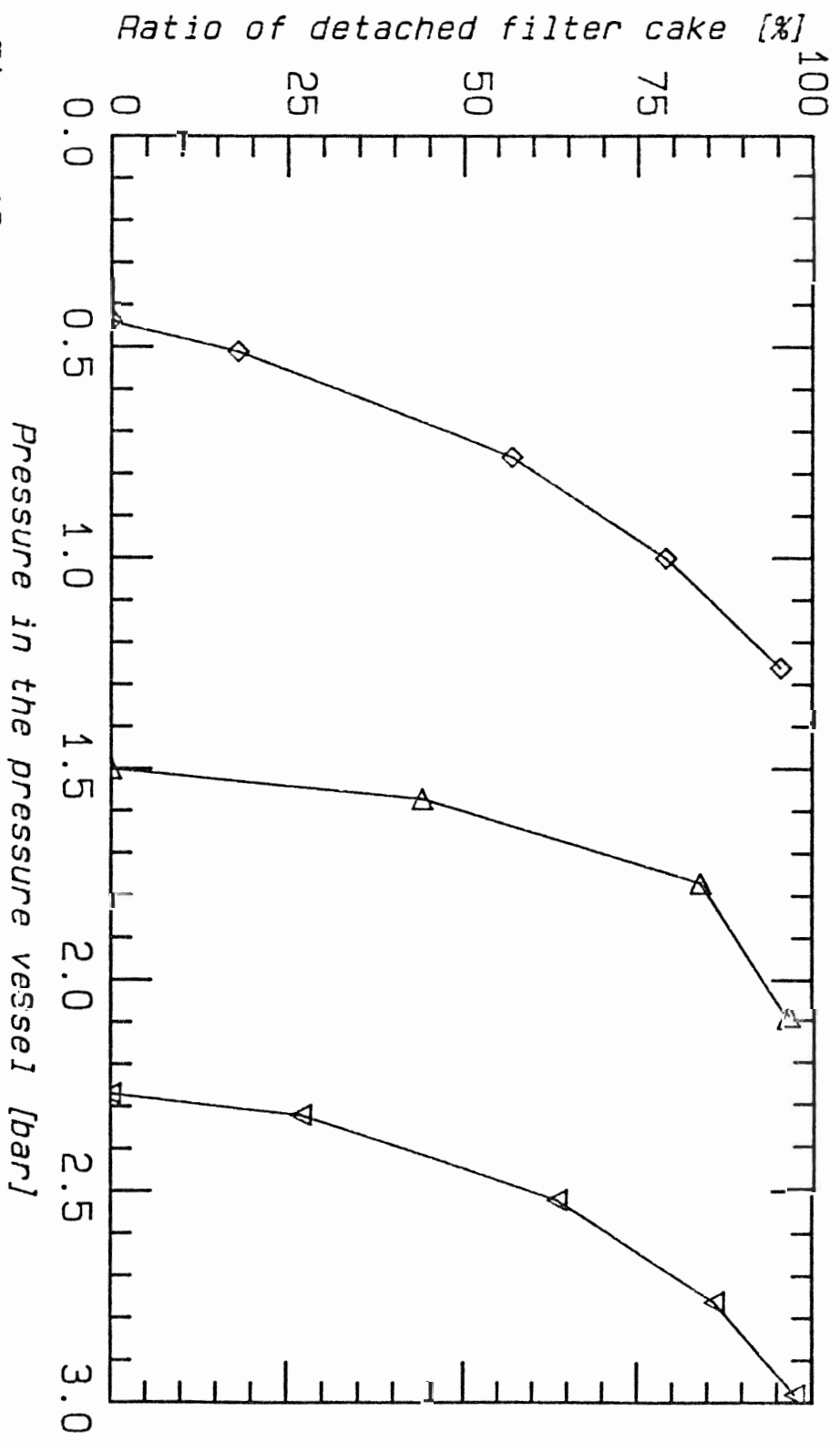


Figure 13:

Experimental results of different filter angles

- ▽ 33° Grad
- △ 20° Grad
- ◇ 10° Grad

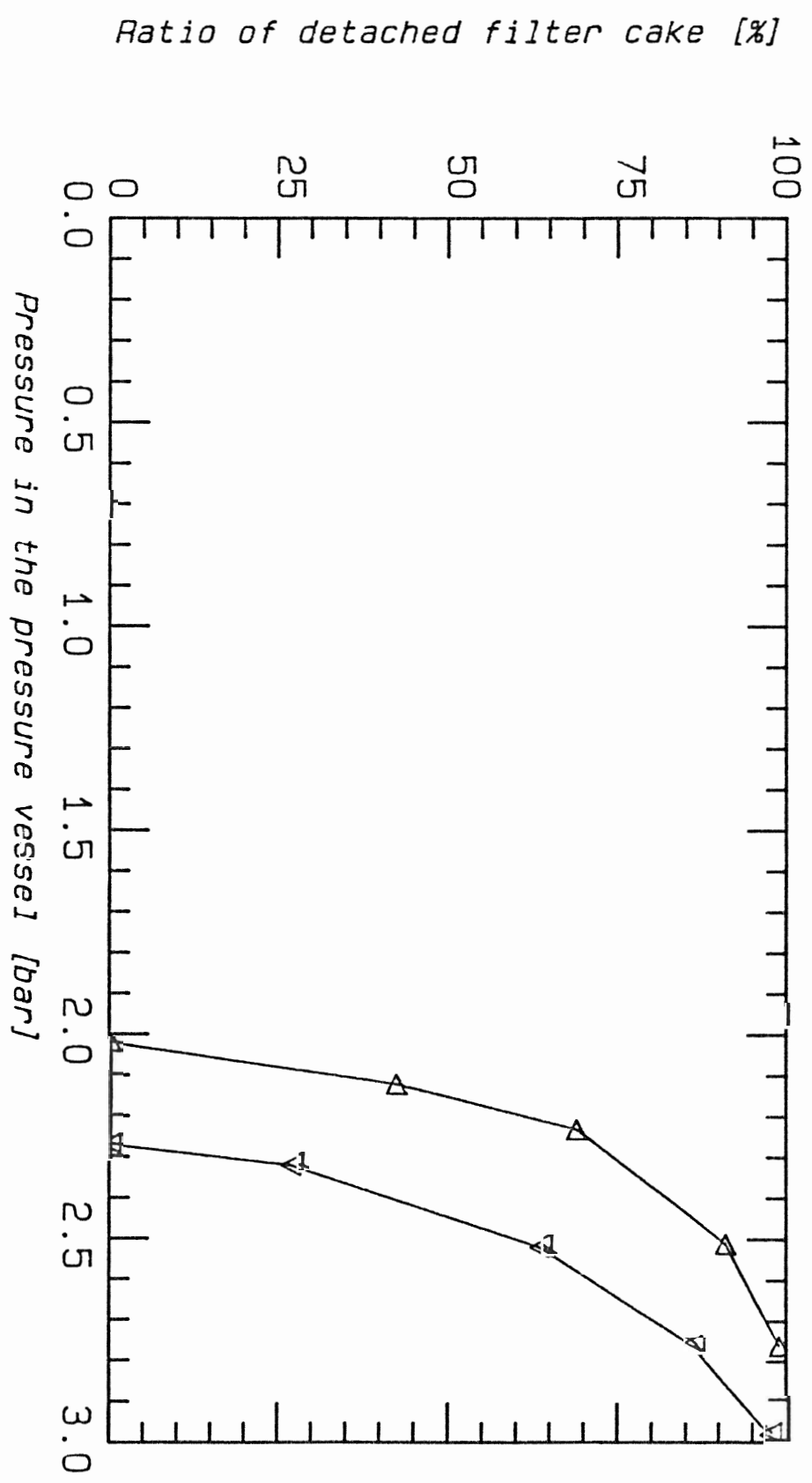


Figure 14:

Experimental results of a fixed filter cloth
 ▽ 33° Grad
 ▲ 33° Grad (fixed filter cloth)

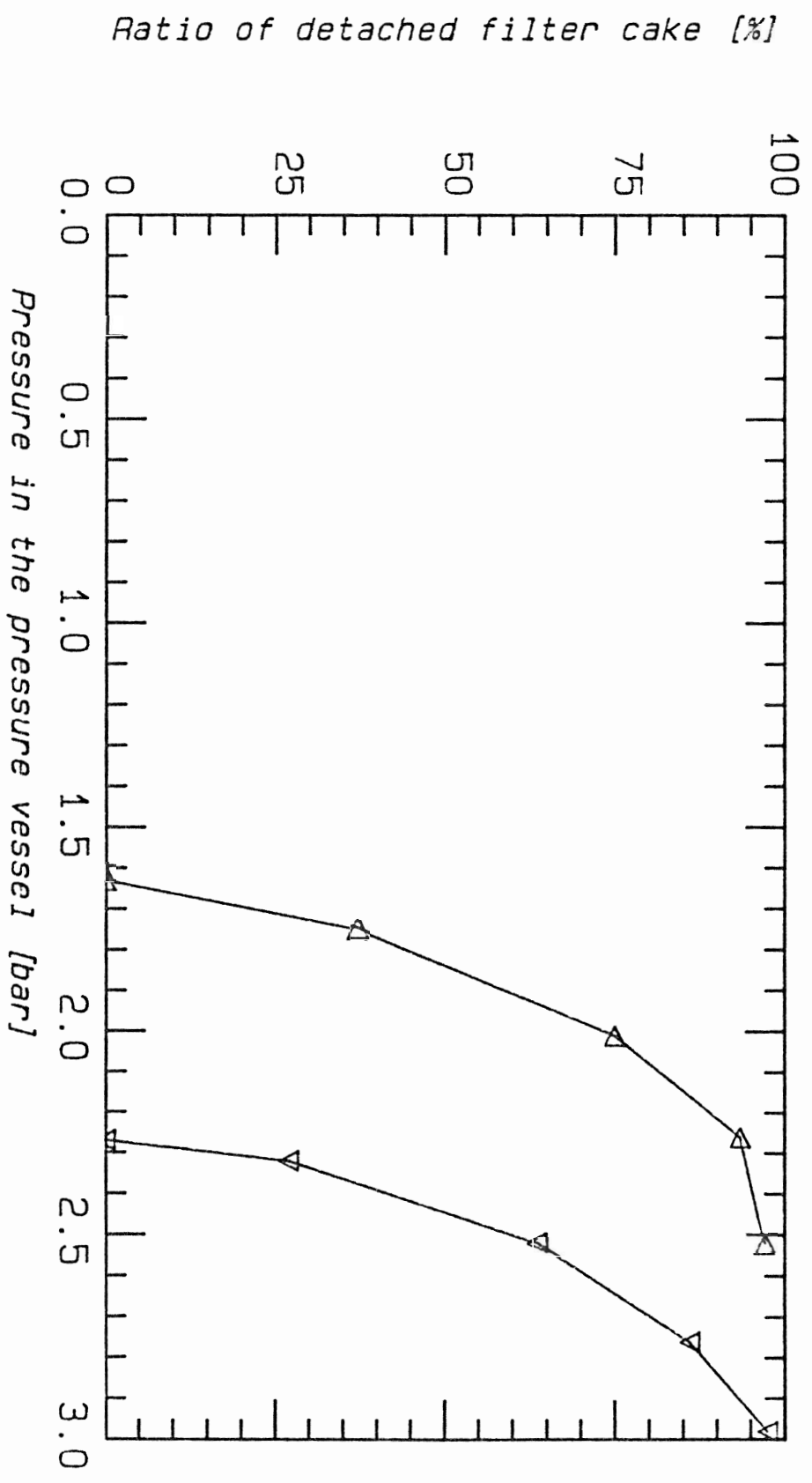


Figure 15:

- Experimental result of a filter cloth with initial stretch
- without initial stretch
- with initial stretch

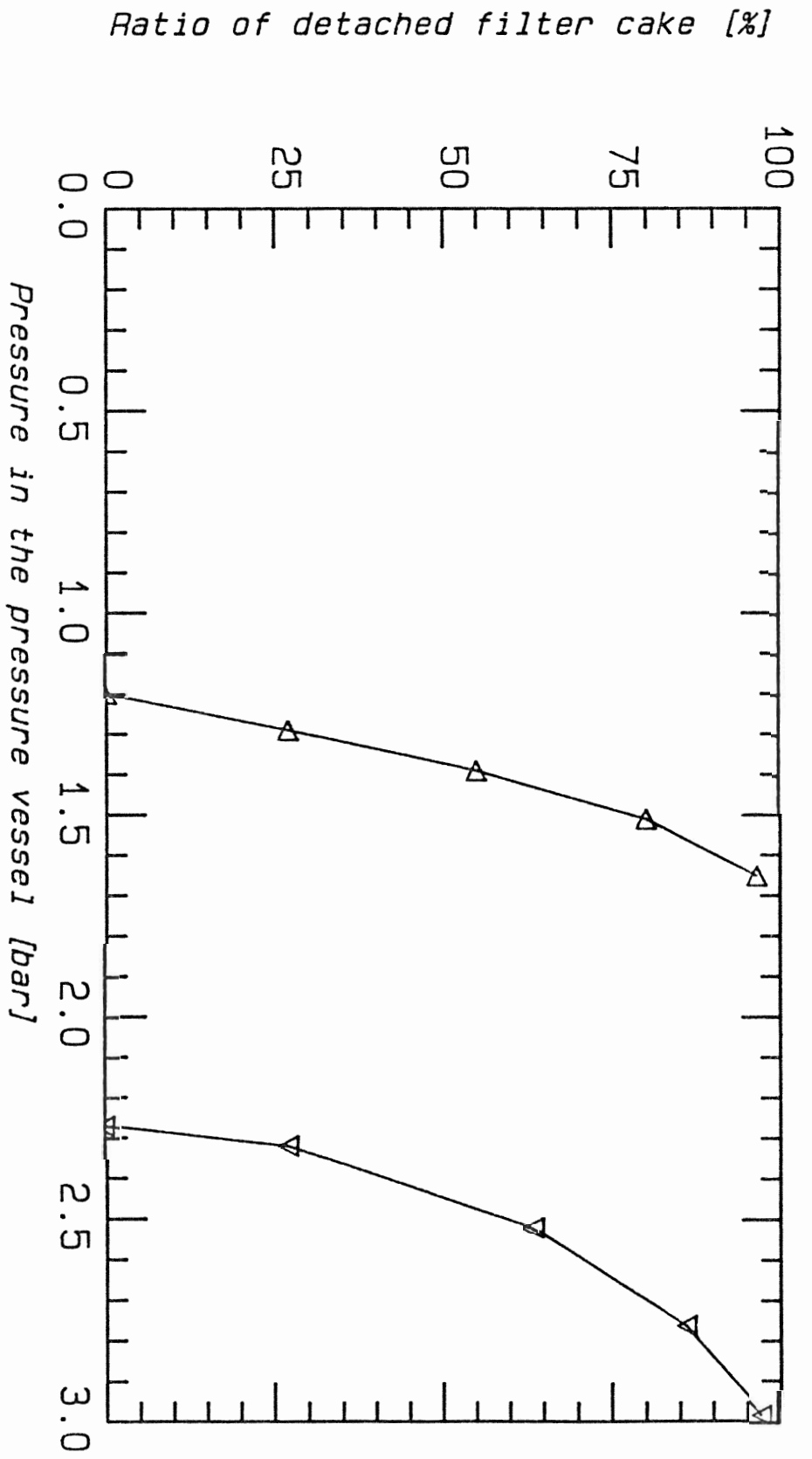


Figure 16:

- Experimental result of a filter cell filled with spheres
- △ filter cell empty
- ▽ filter cell filled up